

# Spectroscopic and Thermodynamic Comparisons of *Escherichia coli* DNA Photolyase and *Vibrio cholerae* Cryptochrome 1

Kathleen Sokolowsky,<sup>†</sup> Maire Newton,<sup>†</sup> Carlos Lucero,<sup>‡</sup> Bradley Wertheim,<sup>†,§</sup>  
 Jaryd Freedman,<sup>†,⊥</sup> Frank Cortazar,<sup>†,||</sup> Jennifer Czocho,<sup>†,#</sup> Johannes P. M. Schelvis,<sup>\*,‡</sup> and  
 Yvonne M. Gindt<sup>\*,†</sup>

Department of Chemistry, Hugel Science Center, Lafayette College, Easton, Pennsylvania 18042, and  
 Department of Chemistry and Biochemistry, Montclair State University, Montclair, New Jersey 07043

Received: March 12, 2010; Revised Manuscript Received: April 16, 2010

*Escherichia coli* DNA photolyase and cryptochrome 1 isolated from *Vibrio cholerae*, a member of the CRY-DASH family, are directly compared using a variety of experimental methods including UV-vis and Raman spectroscopy, reduction potential measurements, and isothermal titration calorimetry. The semiquinone form of the cryptochrome has an absorption spectrum that is red-shifted from that of the photolyase, but the Raman spectrum indicates that the FAD binding pocket is similar to that of photolyase. The FADH<sup>-</sup>/FADH• reduction potential of the cryptochrome is significantly higher than that of the photolyase at 164 mV vs NHE, but it also increases upon substrate binding (to 195 mV vs NHE), an increase similar to what is observed in photolyase. The FADH<sup>-</sup>/FADH• reduction potential for both proteins was found to be insensitive to ATP binding. Isothermal titration calorimetry found that photolyase binds tighter to substrate ( $K_A \sim 10^5 \text{ M}^{-1}$  for photolyase and  $\sim 10^4 \text{ M}^{-1}$  for cryptochrome 1), and the binding constants for both proteins were slightly sensitive to oxidation state. Based upon this work, it appears that this cryptochrome has significant spectroscopic and electrochemical similarities to CPD photolyase. The thermodynamic cycle of the enzymatic repair in the context of this work is discussed.

## Introduction

DNA photolyase and cryptochrome, both members of the blue-light photoreceptor family, are flavoproteins that share sequence and structural homology but appear to play different roles in vivo.<sup>1–6</sup> DNA photolyase has a well-documented role in repair of UV-induced cyclobutylpyrimidine dimers (CPD) in DNA, while the role of cryptochrome, though still poorly understood, appears to be tied to entrainment of circadian rhythms in animals and control of growth and stem elongation in plants. Cryptochrome was defined as a protein that had sequence and structure similarities to DNA photolyase (PL) but lacked DNA repair activity. Both proteins generally contain two cofactors: a flavin adenine dinucleotide (FAD) that is required for activity and a second, nonessential chromophore which is usually a methenyltetrahydrofolate (MTHF).

In 2003, Brudler, Hitomi, Daiyasu, et al., using a combination of phylogenetic, structural, and functional analyses, identified a new subfamily of proteins, the cryptochrome DASH (CRY-DASH) family, that shared common features with the photolyase

subfamily including the ability to bind DNA.<sup>7</sup> Analyzing the crystal structure of a cryptochrome from *Synechocystis* sp. PCC 6803, they found that the protein  $\alpha/\beta$  domains had “high similarity” with the photolyase subfamily structures along with the conservation of the tryptophan triad, three tryptophans that serve to shuttle electrons from the protein surface to the required FAD cofactor which occurs during the photoreduction of the FAD cofactor. This initial work was followed up by a report from Daiyasu, Ishikawa, Kuma, et al. that the CRY-DASH subfamily is widely distributed across all kingdoms of life and that the family displays weak CPD repair activity.<sup>8</sup> Selby and Sancar demonstrated that VcCry1, a member of the subfamily isolated from *Vibrio cholerae*, efficiently repairs single-stranded DNA (ssDNA) but not double-stranded DNA (dsDNA) or RNA.<sup>9</sup> The specific purpose of CRY-DASH is still murky; some work indicates it serves as a transcriptional repressor,<sup>7</sup> while other studies indicate it may serve as a single-strand DNA photolyase with repair of CPD lesions during replication and/or transcription of the DNA.<sup>9,10</sup> Based upon their work, Selby and Sancar recommended that the CRY-DASH family should be reclassified as ssDNA photolyase.<sup>9</sup>

Along with the crystal structure of the protein from *Synechocystis* sp. PCC 6803,<sup>7</sup> crystal structures have been published of cryptochrome 3 (AtCry3) from *Arabidopsis thaliana*,<sup>10–12</sup> another member of the CRY-DASH subfamily. Huang, Baxter, Smith, et al. noted that the AtCry3 appeared to bind MTHF in a manner similar to photolyase, and the presumptive cavity for substrate binding was modified with more charge and less hydrophobic character.<sup>11</sup> In addition, Pokorny, Klar, Hennecke, et al. found that AtCry3 could bind and repair dsDNA if at least one hydrogen bond of the CPD lesion to the complementary strand was perturbed with a significantly distorted double helix,<sup>10</sup> providing some experimental evidence that the protein lacks

\* To whom correspondence should be addressed. Telephone 610-330-5824; fax 610-330-5355; e-mail gindty@lafayette.edu (Y.M.G.); telephone 973-655-3301; fax 973-655-7772; e-mail schelvisj@mail.montclair.edu (J.P.M.S.).

<sup>†</sup> Lafayette College.

<sup>‡</sup> Montclair State University.

<sup>§</sup> Current address: Harvard Medical School, Tosteson Medical Education Center, 760 Longwood Ave., Cannon Society, Boston, MA 02115.

<sup>⊥</sup> Current address: Temple University School of Medicine, Medicine Education and Research Building, 3500 N. Broad Street, Philadelphia, PA 19140.

<sup>||</sup> Current address: University of Miami Miller School of Medicine, Rosenstil Medical Science Building, 1600 NW 10th Ave., Miami, FL 33136.

<sup>#</sup> Current address: Yale University, Biological and Biomedical Sciences, New Haven, CT 06520.

sufficient favorable interactions with dsDNA for a favorable free energy of association.

Several papers have examined the spectroscopy and reduction–oxidation chemistry of the CRY-DASH proteins.<sup>13–17</sup> While class I photolyases are typically isolated with the FAD cofactor in the inactive neutral semiquinone form, the cryptochromes are generally isolated with a fully oxidized FAD cofactor. In contrast, the CRY-DASH proteins appear to be isolated with a large portion of the FAD cofactor in the fully reduced state.<sup>14,15</sup> Clearly, there are differences in the redox behavior of the FAD cofactor for the subfamilies.

In this paper, we build on our previous work<sup>18–21</sup> and directly compare a class I photolyase isolated from *Escherichia coli* with VcCry1, a member of the CRY-DASH family, using variety of experimental methods including UV–vis and Raman spectroscopy, reduction potential measurements, and isothermal titration calorimetry (ITC) measurements. We also examine the thermodynamics of the light-driven electron-transfer repair process in class I photolyase in the context of our findings.

## Experimental Methods

**Isolation of VcCry1 and *E. coli* PL.** The PL was isolated as published earlier<sup>22</sup> and stored at  $-80\text{ }^{\circ}\text{C}$ . The VcCry1 enzyme was produced from *E. coli* strain UNC523F transfected with the pUNC2002 plasmid, a generous gift from Dr. Aziz Sancar at the University of North Carolina. The cells were grown<sup>13</sup> and stored for further use as described.<sup>22</sup>

A typical VcCry1 isolation at  $4\text{ }^{\circ}\text{C}$  is described below. Cell suspension from 8 L of culture is thawed, and the cells are broken by three passes through a Bio-Neb cell nebulizer at a nitrogen pressure between 100 and 150 psi. The suspension is augmented with additional lysis buffer to a minimum of 25 mL of buffer per liter of cells and centrifuged for  $30\text{ min} \times 22\text{ }000\text{ g}$  in a Beckman JA-21 rotor. The resulting pellet of unbroken cells and cell fragments is resuspended and homogenized, and the nebulization is repeated for a second cycle.

The supernatant is treated with ammonium sulfate to 40% saturation (0.243 g/mL). The mixture is spun for 10 min at 22 000 g, and the small pellet is discarded. Additional ammonium sulfate is added to 58% saturation (0.374 g/mL total salt) and centrifuged for 15 min at 22 000 g. The pellet is resuspended in Buffer A (50 mM Hepes, pH 7.0 with 50 mM NaCl, 10 mM BME, 10%(v/v) glycerol). Ammonium sulfate is removed via desalting columns (Bio-Rad, P-6DG polyacrylamide gel) equilibrated with Buffer A.

The desalted liquid is loaded onto a Cibacron Blue 3GA agarose column (Sigma, Type 3000-L, 2.5 cm  $\times$  10 cm) equilibrated in Buffer A. The column is rinsed with Buffer A, and the protein is eluted with 2.00 M KCl in 50 mM Hepes, pH 7.0 with 10 mM BME and 10%(v/v) glycerol. The yellow/green fractions with significant 380 nm (MTHF) absorbance are combined, and the KCl is removed via the desalting columns equilibrated with Buffer B (50 mM Hepes, pH 7.0 with 10 mM NaCl, 10 mM BME, 10%(v/v) glycerol). The desalted solution is immediately loaded onto a Heparin Sepharose CL6B column (GE Healthcare, 2.5 cm  $\times$  12 cm). The column is rinsed with Buffer B and stored overnight at  $4\text{ }^{\circ}\text{C}$ . The yellow-green protein is then eluted as a single band with a linear gradient made from 180 mL of Buffer B and 180 mL of 50 mM Hepes, pH 7.0 with 1.00 M KCl, 10 mM BME, and 10%(v/v) glycerol.

The protein is exchanged into 20 mM potassium phosphate buffer pH 7.0 with 0.40 M  $\text{K}_2\text{SO}_4$  (Buffer M). The protein is concentrated to approximately 300  $\mu\text{M}$  using centrifugal con-

centrators (Amicon Ultra, 30 kD molecular weight cutoff filter) and frozen as individual aliquots at  $-80\text{ }^{\circ}\text{C}$ .

**Preparation of Damaged Substrate.** The oligonucleotides, p(dT)<sub>10</sub> and p(dA)<sub>10</sub>, were purchased from TriLink Biotechnologies and used without further purification. The p(dT)<sub>10</sub> strand was damaged with UV light as described previously.<sup>18</sup> Double-stranded substrate was made by slightly overtitrating damaged p(dT)<sub>10</sub> with p(dA)<sub>10</sub>, as monitored by the absorption spectrum.

**Activity Assay.** Substrate (15  $\mu\text{M}$ ) and enzyme (200 nM) in 50 mM Hepes, pH 7.0 with 10 mM NaCl were combined in a reduced volume quartz fluorescence cuvette equipped with a septum and kept on ice. The solution was purged with  $\text{N}_2$  for 10 min, and 5  $\mu\text{L}$  of fresh sodium dithionite solution (10 mg/mL) was added. The solution was purged for 30 min followed by measurement of the absorption spectrum on a Cary 50 (Varian) spectrometer thermostatted to  $5\text{ }^{\circ}\text{C}$ . The cuvette was then reproducibly placed in a lightproof box equipped with a UVGL-50 mineralight ultraviolet lamp at 1.9 cm from the cuvette at  $4\text{ }^{\circ}\text{C}$ . The sample was illuminated with 365 nm light in 1 min intervals, and the absorption spectrum of the solution was measured to monitor recovery of the DNA. The turnover number of the enzyme was then calculated using the method outlined by Jorns, Sancar, and Sancar.<sup>23</sup>

**Measurement of Reduction Potential for VcCry1.** The reduction potential of VcCry1 was measured as described earlier<sup>19</sup> with the following modifications. The seven mediators used with their midpoint potentials are 1,2-naphthoquinone (180 mV vs NHE), 1,4-naphthoquinone (60 mV), 5-hydroxy-1,4-naphthoquinone (30 mV),  $[\text{Ru}(\text{NH}_3)_6]\text{Cl}_3$  (20 mV), duroquinone (5 mV), 2-hydroxy-1,4-naphthoquinone ( $-145\text{ mV}$ ), and benzyl viologen ( $-348\text{ mV}$ ). The solution potential was measured using a Ag/AgCl reference electrode (3 M KCl, ESA Biosciences) and a Pt working electrode at  $15\text{ }^{\circ}\text{C}$ . The protein was present at 20–35  $\mu\text{M}$  in Buffer M. The mediators were present at 25  $\mu\text{M}$  in the solution, but a range of concentrations from 5 to 50  $\mu\text{M}$  were explored; the concentration used in the measurements was selected since it appeared to be the lowest concentration measured with a reasonable (i.e., 15 min) equilibration time. Each spectrum was corrected for mediator absorption, and the concentration of redox states was calculated using  $\epsilon_{443} = 11\text{ }300\text{ M}^{-1}\text{ cm}^{-1}$  for oxidized enzyme and  $\epsilon_{630} = 4150\text{ M}^{-1}\text{ cm}^{-1}$  for neutral semiquinone.

**Cleavage of the Maltose Binding Domain from VcCry1.** The MBD was cleaved from VcCry1 using 0.02 activity units of restriction grade bovine factor Xa (Novagen) per microgram of MBP-VcCry1 in Buffer M at  $4\text{ }^{\circ}\text{C}$ . The reaction was monitored by SDS-PAGE, not shown, with no evidence of secondary proteolysis and apparent complete cleavage in 24 h. Aliquots of the reaction mixture were removed at regular intervals for 48 h, and the activity and the absorption spectrum of VcCry1 in the reaction mixture were compared to control MBP-VcCry1 (protein under identical conditions with the absence of the cleavage enzyme).

**Resonance Raman Experiments.** The resonance Raman experiments were performed on the instrument described previously.<sup>24</sup> A 532 nm diode-pumped solid state (DPSS) laser (Lambda Pro) and a 561 nm DPSS laser (CrystaLaser) were used as excitation sources. The laser intensity was approximately 15 mW at the sample. The samples were contained in Raman spinning cells and kept at  $7 (\pm 3)\text{ }^{\circ}\text{C}$  for the duration of the experiments. PL with FADH• was diluted to 250  $\mu\text{M}$  using Buffer M. VcCry1 with FADH• was prepared by purging a 250  $\mu\text{M}$  solution with nitrogen followed by the addition of sodium

dithionite to a final concentration of 1.6 mM. After reduction of VcCry1 to the FADH<sup>-</sup> state was complete, potassium ferricyanide was added to a final concentration of 2.8 mM to obtain VcCry1 with FADH•. For the VcCry1 experiments with UV-p(dT)<sub>10</sub>, UV-p(dT)<sub>10</sub> was added to a final concentration of about 800 μM, giving a 3:1 ratio of UV-p(dT)<sub>10</sub> and VcCry1. FADH• was stable for the duration of the experiment (30–60 min) in both PL and VcCry1. Toluene was used to calibrate the Raman spectrophotometer, and spectra of reduced and oxidized VcCry1 were collected to correct the baseline for emission from trace amounts of FADH<sup>-</sup> and FAD present in the samples. If necessary, a smooth polynomial was used to correct the baseline.

**Isothermal Titration Calorimetry Measurements.** Binding studies were done at 10 °C with a MicroCal ITC<sub>200</sub> microcalorimeter (GE Biosciences) using enzyme in the sample cell at concentrations of 100–170 μM and substrate in the titration syringe at concentrations of 1.8–2.9 mM. Both the protein and DNA substrate were in Buffer M, and the substrate was added in 20–24 aliquots with 90–120 s per addition and a 1000 rpm stir rate. Three molecules were used as titrants: UV-p(dT)<sub>10</sub>, a double-strand DNA of UV-p(dT)<sub>10</sub> and p(dA)<sub>10</sub>, and undamaged p(dT)<sub>10</sub>. Each titration took approximately 1 h.

The PL was taken directly from the -80 °C freezer in the semiquinone form, while oxidized PL was produced by incubating PL overnight at 4 °C with a 1000 molar excess of potassium ferricyanide in Buffer M. The excess potassium ferricyanide was removed from the sample using three cycles of concentration and dilution with additional Buffer M in centrifugal concentrators. Fully oxidized VcCry1 was produced by allowing the protein in Buffer M to sit at room temperature for 2 h open to the atmosphere. The VcCry1 semiquinone form was produced as described earlier for the Raman studies.

It was necessary to run the ITC titrations with relatively high enzyme and substrate concentrations to get data with sufficient signal-to-noise. In addition, two sets of controls were run for each enzyme. First, the DNA was titrated into Buffer M to correct for the heat of the dilution of the DNA. Second, Buffer M was titrated into the protein to correct for the heat of dilution of the protein. The controls were subtracted from the titration data with one exception; the heat of dilution of the VcCry1 semiquinone state was so small that it was ignored. The data was analyzed using a one-site binding model with the Origin package and propriety software that came with the ITC.

## Results

The VcCry1 and PL proteins were isolated in similar procedures, and differences in the reduction–oxidation properties of the two flavoproteins were readily apparent since the PL protein was consistently seen as a blue solution (indicating neutral semiquinone) while the VcCry1 early in the prep was mostly yellow (as fully reduced FAD) and later as a green solution with an absorption spectrum that indicated the presence of all three oxidation states. In addition, we also noticed that our VcCry1 samples would oxidize upon storage in a -80 °C freezer; the PL semiquinone state is stable for years at the same storage temperature.

The VcCry1 was isolated with a maltose binding domain (MBD). To determine if the MBD was modifying the behavior of the protein, we cleaved the domain and compared the cleavage product to VcCry1 with MBD attached. There were no discernible differences in either the qualitative redox chemistry or the activities of the enzyme with the MBD absent. Therefore, for all further studies discussed in this paper, the VcCry1 protein has the MBD present.

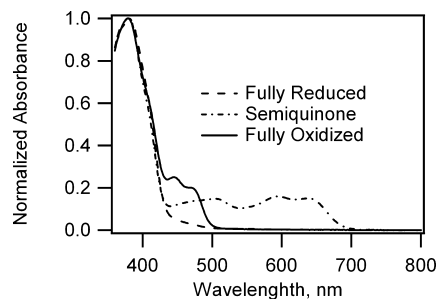


**Figure 1.** Absorption spectra of the three oxidation states of VcCry1 normalized to 380 nm.

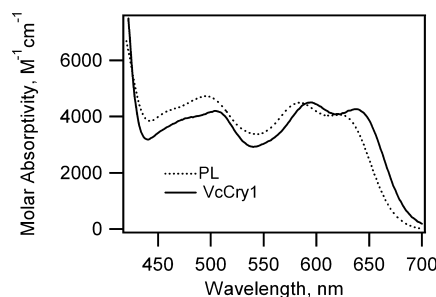


**Figure 2.** Comparison of the absorption spectra of the FADH• states for PL and VcCry1.

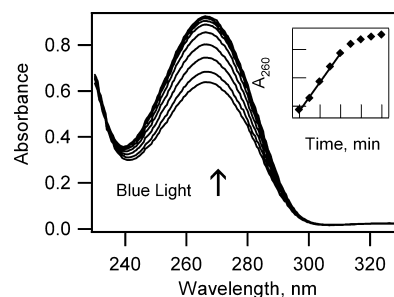


**Figure 3.** Typical activity assay used to calculate the turnover number of the enzyme. The absorbance at 260 nm increases upon absorption of blue light. The 260 nm absorbance is plotted against the illumination time, shown in the inset. The turnover number is calculated from the slope of the line, as described in the text.

## Chromophore Content and Absorption Spectroscopy.

Using the procedures described in the literature,<sup>25,26</sup> we determined the ratio of the FAD to the MTHF chromophore and found a 1:1 molar ratio within the error of the method. Earlier, we found the FAD to MTHF molar ratio of 1:0.6 for the PL protein isolated using our procedure.<sup>18,21</sup> We determined extinction coefficients for the VcCry1 protein for two oxidation states. The fully oxidized state appears to have an  $\epsilon_{443} = 11\,300\text{ M}^{-1}\text{ cm}^{-1}$ , in agreement with earlier work,<sup>13</sup> while the neutral semiquinone has  $\epsilon_{590} = 4500 (\pm 200)\text{ M}^{-1}\text{ cm}^{-1}$  and  $\epsilon_{630} = 4150 (\pm 200)\text{ M}^{-1}\text{ cm}^{-1}$ . The absorption spectra of the three oxidation states of VcCry1 are shown in Figure 1; for easier comparison, the spectra are normalized at 380 nm. The spectrum of the VcCry1 semiquinone was found to be red-shifted by approximately 30 nm from that of the PL semiquinone, Figure 2, similar to what was observed for Zebrafish CRY-DASH by Zikihara, Ishikawa, Todo, and Tokutomi<sup>16</sup>

**Activity Assays.** We compared the activities of the enzymes with typical data shown in Figure 3. We found PL to have a turnover number of  $13\text{ min}^{-1} (\pm 1\text{ min}^{-1}, 3\text{ trials})$  and  $4.4\text{ min}^{-1} (\pm 0.9\text{ min}^{-1}, 6\text{ trials})$  for ssDNA and dsDNA, respectively. Under identical conditions with identical substrates, VcCry1 had turnover numbers of  $14\text{ min}^{-1} (\pm 1\text{ min}^{-1}, 5\text{ trials})$  and  $8\text{ min}^{-1}$

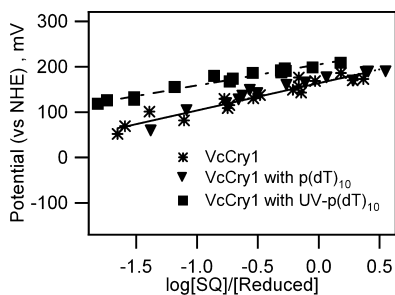


**Figure 4.** Nernst plots obtained for VcCry1 for the FADH<sup>•</sup>/FADH<sup>-</sup> reduction potential. Three sets of data are overlaid, including VcCry1 alone, VcCry1 in the presence of 13× molar excess of UV-p(dT)<sub>10</sub>, and VcCry1 in the presence of 120× molar excess of Mg-ATP.

(±2 min<sup>-1</sup>, 7 trials) for ssDNA and dsDNA, respectively. The turnover numbers of the dsDNA substrate may be slightly underestimated since we used a molar absorptivity at 266 nm of 8300 M<sup>-1</sup> cm<sup>-1</sup><sup>23</sup> for the recovery of the thymine base, the same number used with ssDNA.

**Measurement of Reduction Potentials.** We were unable to measure the one-electron reduction potential of the FADH<sup>•</sup> to fully reduced FADH<sup>-</sup> state in VcCry1 using the conditions we developed previously for PL.<sup>19</sup> We changed to a new set of mediators for two reasons: the VcCry1 reduction potential was significantly higher than what we had measured for PL, and we gained significant turbidity over the course of the experiment. We increased the temperature from 10 to 15 °C since the VcCry1 appeared to have equilibration problems at 10 °C.

Using the method of analysis as previously described by Dutton,<sup>27</sup> we measured the FADH<sup>-</sup>/FADH<sup>•</sup> midpoint potential at 164 mV (±3 mV, 4 trials) vs NHE with an average slope of 60 mV on the Nernst plot, typical data shown in Figure 4. In the presence of a 13 times molar excess of UV-p(dT)<sub>10</sub> substrate, the reduction potential increased to 195 mV (±4 mV, 4 trials). The measured potential with the same excess of undamaged p(dT)<sub>10</sub> was 160 mV (average of 2 trials), unchanged from enzyme alone. We also found the reduction potential of both VcCry1 and PL to be unchanged in the presence of 120× molar excess of Mg-ATP, data not shown.

Although we did not quantify this effect, in the VcCry1 solutions that contained either excess UV-p(dT)<sub>10</sub> or Mg-ATP, less FAD<sub>ox</sub> was produced during the course of these titrations, but this effect was not seen with the undamaged p(dT)<sub>10</sub>. Although our titrations produced significant amounts of fully oxidized protein, we were unable to fully titrate the FADH<sup>•</sup> state to the FAD<sub>ox</sub> state. As the potential of the solution increased, the time required for equilibration increased with the solution mixture taking more than an hour to equilibrate. This effect was also noted in a qualitative study of the redox properties of CRY-DASH from *Synechocystis*.<sup>17</sup>

**Isothermal Titration Calorimetry.** We obtained ITC data, Table 1, for both proteins using ssDNA (UV-p(dT)<sub>10</sub>), dsDNA (UV-p(dT)<sub>10</sub> bound to p(dA)<sub>10</sub>), or undamaged DNA in Buffer M since both enzymes displayed exceptional stability in this solvent system. In addition, we investigated substrate binding for two oxidation states of the proteins: the FADH<sup>•</sup> state and the FAD<sub>ox</sub> state. Since the fully reduced state is harder to maintain under an oxygen atmosphere, we do not have data for the fully reduced forms of the enzymes. Approximately 95% of the enzyme survived the titration in its initial redox state for PL FADH<sup>•</sup>, PL FAD<sub>ox</sub>, and VcCry1 FAD<sub>ox</sub>; 85–95% of the VcCry1 FADH<sup>•</sup> survived the titration. This assessment was based upon the absorption spectrum of the protein before and after each titration.

As shown in Figure 5B and 5D, we obtained association constants  $K_A = 1.45 \times 10^5 \text{ M}^{-1}$  and  $K_A = 1.75 \times 10^5 \text{ M}^{-1}$  for ssDNA and dsDNA substrate binding to the FADH<sup>•</sup> state of PL. The enthalpy of binding for the semiquinone PL was found to be more negative for the dsDNA substrate with  $\Delta H^\circ = -6300$  and  $-4960 \text{ cal/mol}$  for dsDNA and ssDNA substrate, respectively. We also obtained binding data for the oxidized form of PL with  $K_A = 1.11 \times 10^5 \text{ M}^{-1}$  and  $\Delta H^\circ = -4000 \text{ cal/mol}$  with ssDNA substrate, Figure 5F.

We repeated the binding experiments using VcCry1 with identical substrates. We found an association constant of  $3.8 \times 10^4 \text{ M}^{-1}$  for the FADH<sup>•</sup> state with  $\Delta H^\circ = -2800 \text{ cal/mol}$  with ssDNA substrate, Figure 6B. The fully oxidized enzyme appears to have  $K_A = 2.6 \times 10^4 \text{ M}^{-1}$  with  $\Delta H^\circ = -1900 \text{ cal/mol}$  for binding of ssDNA substrate, Figure 6F. The error bars on the association constant and enthalpy value for the FADH<sup>•</sup> state of VcCry1 are relatively large, and this is most likely due to 5%–15% of the FADH<sup>•</sup> state being lost over the course of the titration. The ITC data for VcCry1 FADH<sup>•</sup> with dsDNA substrate is clearly much different than what was observed earlier with PL FADH<sup>•</sup>, Figure 6C and 6D, and the binding curve is significantly altered.

We also titrated both PL and VcCry1 FADH<sup>•</sup> state with undamaged ssDNA and measured only weak binding with an association constant of approximately  $10^2 \text{ M}^{-1}$ . All the experiments described above were corrected for both dilution of the DNA titrant and dilution of the enzyme with the exception of the VcCry1 FADH<sup>•</sup> state. The oxidized VcCry1 displayed anomalous behavior; it was the only protein that displayed a large exothermic enthalpy of dilution, Figure 6E.

**Raman Spectroscopy.** Resonance Raman spectra of FADH<sup>•</sup> in PL and in VcCry1 with excitation at 532 and 561 nm are shown in Figure 7A and 7B, respectively. The resonance Raman spectrum of FADH<sup>•</sup> in VcCry1 is nearly identical to that in PL.<sup>18,29,30</sup> The most significant difference is in the band at 1227 cm<sup>-1</sup>, which occurs at 1222 cm<sup>-1</sup> in PL. A second, less discernible difference is in the band at 1351 cm<sup>-1</sup>, which occurs 4 cm<sup>-1</sup> higher and with weaker intensity compared to PL. There are also some small differences in relative intensities of the resonance Raman bands of FADH<sup>•</sup> in PL and in VcCry1, most likely due to the red-shifted absorption spectrum of FADH<sup>•</sup> in VcCry1 (Figure 2) causing a small difference in the resonance Raman excitation profile. For example, the bands at 1260 and 1331 cm<sup>-1</sup> are relatively weaker in VcCry1 following excitation at 561 nm. Since these two bands are enhanced by excitation of the D<sub>0</sub> → D<sub>1</sub> transition,<sup>18</sup> the red-shift of the FADH<sup>•</sup> absorption band in VcCry1 explains the lower relative intensities of these Raman bands.

Substrate binding to VcCry1 induces several reproducible changes in the position and intensity of the Raman bands of FADH<sup>•</sup>. These changes are more pronounced than those for binding of UV-p(dC)<sub>10</sub> to PL<sup>20</sup> but less pronounced than those observed for UV-p(dT)<sub>10</sub> binding to PL.<sup>18</sup> Two key changes that were observed for substrate binding to PL are also detected for substrate binding to VcCry1. First, the relative intensities of the bands at 1303 and 1331 cm<sup>-1</sup> become equal. This is very similar to what was observed for substrate binding to PL<sup>18</sup> and provides evidence that substrate is bound to VcCry1 under our experimental conditions. Second, it appears that the H-bonding sensitive band at 1351 cm<sup>-1</sup> in VcCry1 (1347 cm<sup>-1</sup> in PL) shifts or disappears. This observation is somewhat hindered due to the quality of the resonance Raman spectrum of substrate-bound VcCry1, which was affected by the presence of a low-concentration luminescent contaminant in the UV-p(dT)<sub>10</sub>.

TABLE 1: Comparison of Enzymatic and Thermodynamic Values

quantity	<i>E. coli</i> photolyase	VcCry1
turnover number with ssDNA <sup>a</sup>	13 ( $\pm 1$ ) min <sup>-1</sup>	14 ( $\pm 1$ ) min <sup>-1</sup>
turnover number with dsDNA <sup>b</sup>	4.4 ( $\pm 0.9$ ) min <sup>-1</sup>	8 ( $\pm 2$ ) min <sup>-1e</sup>
$E^\circ$ (FADH•/FADH <sup>-</sup> ) no substrate <sup>c</sup>	0 ( $\pm 6$ ) mV <sup>d</sup>	164 ( $\pm 3$ ) mV
$E^\circ$ (FADH•/FADH <sup>-</sup> ) with ssDNA <sup>c</sup>	65 ( $\pm 8$ ) mV <sup>d</sup>	195 ( $\pm 4$ ) mV
$K_A$ (FADH• with ssDNA)	$1.45 (\pm 0.05) \times 10^5 \text{ M}^{-1}$	$3.8 (\pm 2) \times 10^4 \text{ M}^{-1}$
$K_A$ (FADH• with dsDNA)	$1.8 (\pm 0.1) \times 10^5 \text{ M}^{-1}$	N/A <sup>e</sup>
$K_A$ (FAD <sub>ox</sub> with ssDNA)	$1.11 (\pm 0.07) \times 10^5 \text{ M}^{-1}$	$2.6 (\pm 0.8) \times 10^4 \text{ M}^{-1}$
$\Delta H^\circ_{\text{binding}}$ (FADH• with ssDNA)	-4960 ( $\pm 60$ ) cal/mol	-2800 ( $\pm 400$ ) cal/mol
$\Delta H^\circ_{\text{binding}}$ (FADH• with dsDNA)	-6300 ( $\pm 400$ ) cal/mol	N/A <sup>e</sup>
$\Delta H^\circ_{\text{binding}}$ (FAD <sub>ox</sub> with ssDNA)	-4000 ( $\pm 200$ ) cal/mol	-1900 ( $\pm 400$ ) cal/mol
$\Delta G^\circ_{\text{binding}}$ (FADH• with ssDNA)	-6680 ( $\pm 20$ ) cal/mol	-5900 ( $\pm 300$ ) cal/mol
$\Delta G^\circ_{\text{binding}}$ (FADH• with dsDNA)	-6800 ( $\pm 300$ ) cal/mol	N/A <sup>e</sup>
$\Delta G^\circ_{\text{binding}}$ (FAD <sub>ox</sub> with ssDNA)	-6530 ( $\pm 40$ ) cal/mol	-5700 ( $\pm 200$ ) cal/mol
$\Delta S^\circ_{\text{binding}}$ (FADH• with ssDNA)	6.1 cal/K mol	11 cal/K mol
$\Delta S^\circ_{\text{binding}}$ (FADH• with dsDNA)	1.8 cal/K mol	N/A <sup>e</sup>
$\Delta S^\circ_{\text{binding}}$ (FAD <sub>ox</sub> with ssDNA)	9.0 cal/K mol	13 cal/K mol

<sup>a</sup> ssDNA substrate is UV-p(dT)<sub>10</sub>. <sup>b</sup> dsDNA substrate is UV-p(dT)<sub>10</sub> with p(dA)<sub>10</sub>. <sup>c</sup> Versus NHE standard. <sup>d</sup> Slightly revised value from ref 19 to reflect modified correction for Ag/AgCl electrode. <sup>e</sup> dsDNA appears to be disrupted upon binding of VcCry1.

## Discussion

**Implications of the Redox Measurements.** We found VcCry1 to have a FADH<sup>-</sup>/FADH• reduction potential of 164 ( $\pm 3$ ) mV vs NHE in the absence of substrate compared to PL and that it also undergoes an increase to 195 ( $\pm 4$ ) mV with UV-p(dT)<sub>10</sub> substrate bound. In our earlier work on PL,<sup>19</sup> we used a correction factor of 231 mV to convert our reduction potentials measured with the Ag/AgCl reference electrode to the NHE standard. A factor of 215 mV is more accurate for our specific experimental conditions and temperature,<sup>31</sup> and, thus, our measurement for the FADH•/FADH<sup>-</sup> couple in PL needs to be revised slightly to 0 ( $\pm 6$ ) mV for the PL alone and 65 ( $\pm 8$ ) mV for the PL in the presence of UV-p(dT)<sub>10</sub> substrate. Others have measured the FADH•/FADH<sup>-</sup> couple in PL at 40 mV (substrate bound, pH 7.5)<sup>32</sup> and at -48 mV (no substrate, pH 7.4) and 28 mV (substrate bound, pH 7.4).<sup>14</sup>

There are two reported values for cryptochrome reduction potentials in the literature; a paper by Lin, Robertson, Ahmad, et al. reported that the  $E_2$  midpoint potential of cryptochrome 1 from *Arabidopsis thaliana* (AtCry1) was -181 mV at pH 8.0.<sup>33</sup> There was a second published measurement for AtCry1 at pH 7.0 with the  $E_2$  midpoint potential (FADH• to FADH<sup>-</sup>) at -161 mV and  $E_1$  (FAD to FADH•) at -153 mV.<sup>14</sup> Balland, Byrdin, Eker, et al. proposed that the plant cryptochromes evolved to have a lower  $E_1$  (FAD to FADH•) redox potential since the FAD and FADH• states appear to be critical as “dark” and “signaling” states, respectively; in contrast, PL requires the fully reduced FADH<sup>-</sup> for repair of the DNA.<sup>14</sup> Based upon this reasoning, our  $E_2$  redox measurement for VcCry1, which is 300 mV higher than that measured for AtCry1,<sup>14</sup> favors a role of the fully reduced FADH<sup>-</sup> cofactor in the CRY-DASH proteins either for DNA repair or for signaling with fully reduced flavin. This is consistent with our observation that the enzyme is initially isolated in the fully reduced form from the cells. This may be a risky interpretation since the VcCry1  $E_1$  couple may be too close to the  $E_2$  couple as we observe fully oxidized flavin during the  $E_2$  redox titration; this is similar to the observations noted for AtCry1<sup>14,17</sup> but unlike the PL enzyme.

There are a number of factors that may tune the redox potentials of flavoproteins including aromatic stacking, hydrogen bonding, dehydration, and flavin bending.<sup>34–39</sup> We believe that the most likely explanation for the increase in the  $E_2$  potential for PL in the presence of the substrate is the  $\sim 9^\circ$  bend in the isoalloxazine ring detected with the substrate bound.<sup>20,40</sup> We

examined the FAD cofactor in two crystal structures (2VTB and 2J4D) recently published for the CRY-DASH protein, AtCry3, with and without substrate analogue bound.<sup>10,12</sup> With the substrate bound, the isoalloxazine ring is planar while in the absence of the substrate, the two nitrogens in the center ring are 0.18 Å out of the plane as judged by a plane created by the four outermost atoms using the Mercury CSD 2.3 (Build RC4) viewing package. This effect is opposite of what is observed with PL, so the increase in the  $E_2$  midpoint potential observed upon binding of the substrate to VcCry1 is not consistent with bending of the isoalloxazine ring on the basis of the AtCry3 crystallographic data.

Brudler, Hitomi, Daiyasu, Toh, et al. reported only a few significant differences in the FAD binding pocket with photolyase and *Synechocystis* CRY-DASH; two trp (Trp271 and Trp338 in PL) side chain hydrogen bonds to FAD phosphate oxygen are not present in CRY-DASH, while a new hydrogen bond forms between Asn395 to the NH<sub>2</sub> group and the ring nitrogen of the adenine base in CRY-DASH.<sup>7</sup> Although changes in the hydrogen bonds to the adenine base may play some role in the observed differences in the redox potentials, contacts with the isoalloxazine ring may be more important.

There have been reported effects of ATP on plant cryptochrome redox chemistry.<sup>41</sup> We found no discernible effects of ATP on the thermodynamics of the oxidation of FADH<sup>-</sup>, but the presence of ATP does decrease the concentration of fully oxidized VcCry1 during the  $E_2$  titration. Immeln, Schlesinger, Heberle, and Kottke noted that binding of ATP to *Chlamydomonas* cry protected the semiquinone state of the protein against oxidation by O<sub>2</sub>.<sup>41</sup> We observed a similar effect in VcCry1 with the addition of either excess Mg-ATP or UV-p(dT)<sub>10</sub>, but only the UV-p(dT)<sub>10</sub> proved to have any measurable effect on the  $E_2$  midpoint potential. We hypothesize that addition of ATP may increase the  $E_1$  midpoint potential or may slow down the kinetics of the oxidation, perhaps by blocking access to the FAD cofactor through conformational changes.

**FADH• Environment in VcCry1.** The resonance Raman spectra of VcCry1 provide insight into the FADH• binding pocket of VcCry1. Although it has been reported that the CRY-DASH family has more sequence homology with (6–4) photolyases than with CPD photolyases,<sup>7</sup> the resonance Raman spectrum of FADH• in VcCry1 is very similar to that of *E. coli* photolyase, a CPD photolyase, and quite different from that of *A. thaliana* (6–4) photolyase.<sup>16,29,30,42</sup> This strongly suggests that

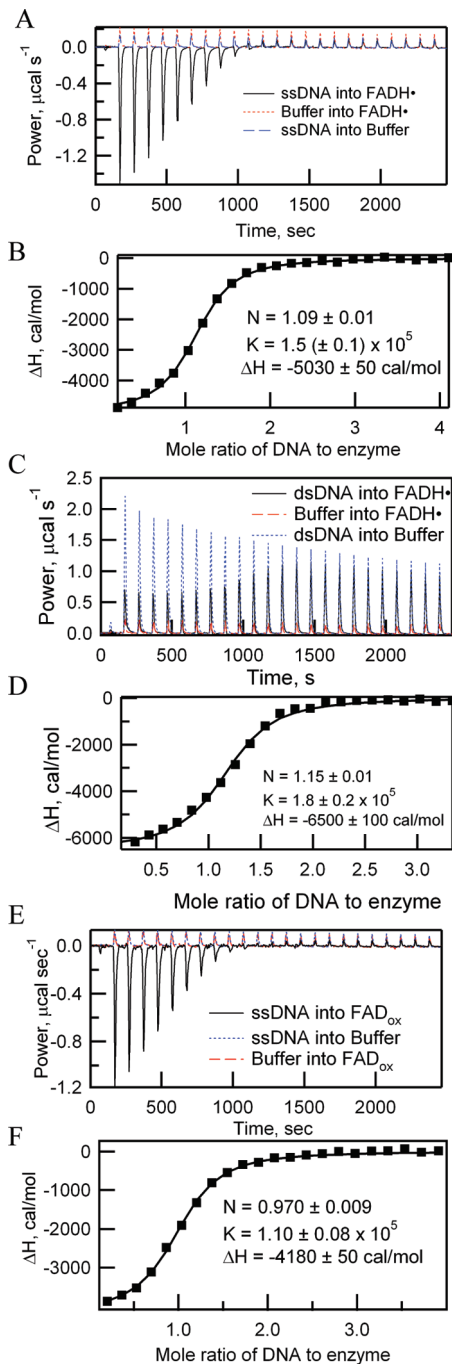


**Figure 5.** ITC and binding curves obtained for PL with different titrants. Experimental conditions are described in the text. Each ITC graph contains three sets of data obtained under identical conditions: the titrant added to enzyme, titrant added to buffer (correction for dilution of titrant), and buffer added to enzyme (correction for dilution of enzyme). The binding curves have been corrected for the dilutions. The parameters obtained by fitting the binding curve to a one-site model are given for the specific data shown. (A, B) ITC and binding curve for UV-p(dT)<sub>10</sub> to the FADH• state of PL. (C, D) ITC and binding curve for dsDNA to the FADH• state of PL. (E, F) ITC and binding curve for UV-p(dT)<sub>10</sub> to the FAD<sub>ox</sub> state of PL.

the FADH• binding pocket in *VcCry1* is very similar to the one in PL with similar contacts made between FADH• and the protein matrix, in agreement with crystallography results.<sup>7,10–12</sup> There are two significant differences: first, the weak band at 1351 cm<sup>-1</sup> occurs at 1347 cm<sup>-1</sup> in PL and has been shown to be sensitive to hydrogen bonding.<sup>18</sup> The 4 cm<sup>-1</sup> shift in this band may indicate that hydrogen bonding to N<sub>3</sub>H and/or N<sub>5</sub>H

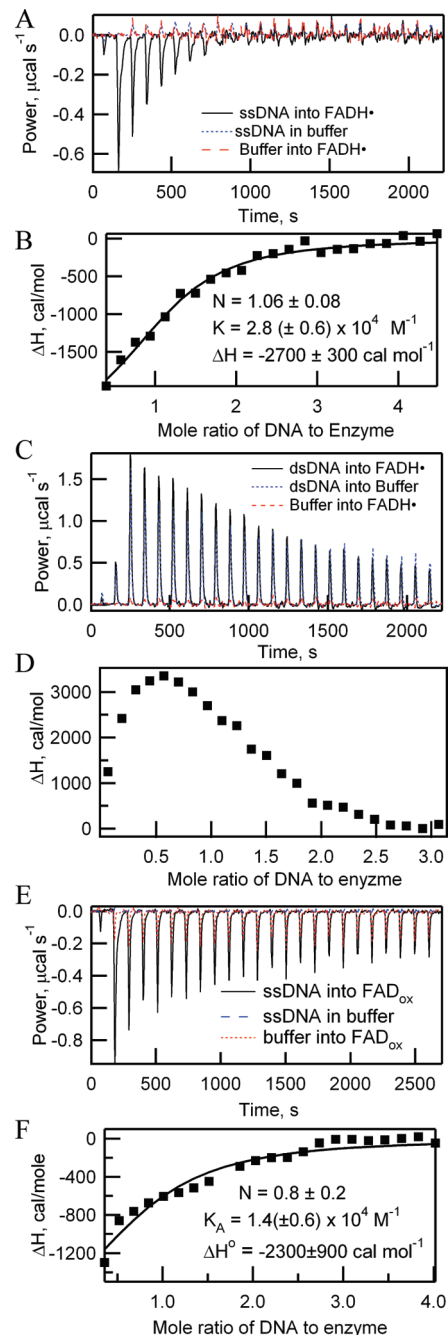


**Figure 6.** ITC and binding curves obtained for *VcCry1* with different titrants. Experimental conditions are described in the text. Each ITC graph contains three sets of data obtained under identical conditions: the titrant added to enzyme, titrant added to buffer (correction for dilution of titrant), and buffer added to enzyme (correction for dilution of enzyme). The binding curves have been corrected for the dilutions. The parameters obtained by fitting the binding curve to a one-site model are given for the specific data shown. (A, B) ITC and binding curve for UV-p(dT)<sub>10</sub> to the FADH• state of *VcCry1*. (C, D) ITC and binding curve for dsDNA to the FADH• state of *VcCry1*. (E, F) ITC and binding curve for UV-p(dT)<sub>10</sub> to the FAD<sub>ox</sub> state of *VcCry1*.

of FADH• in *VcCry1* is slightly different than in *E. coli* PL. A corresponding band has not been reported for *A. thaliana* (6–4) photolyase,<sup>30,42</sup> probably because 568.1 nm was used for excitation rather than 532 nm, which is necessary to enhance this band. Second, the band that occurs at 1227 cm<sup>-1</sup> in *VcCry1* is observed at 1222 cm<sup>-1</sup> in *E. coli* PL and at 1220 cm<sup>-1</sup> in *A. thaliana* (6–4) photolyase.<sup>42</sup> Although this band may be an interesting marker to differentiate the various enzymes, its origin

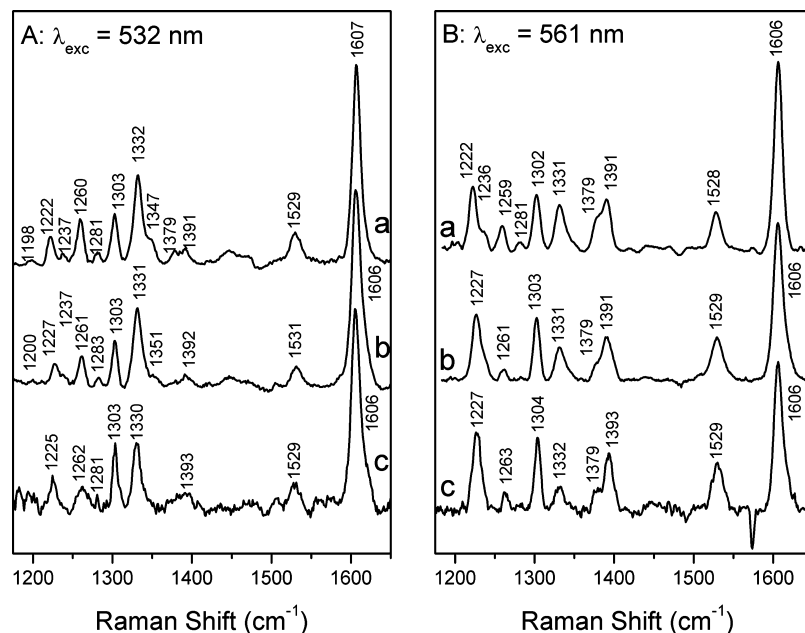


**Figure 7.** High-frequency resonance Raman spectra of FADH• in (a) *E. coli* photolyase, (b) VcCry1, and (c) VcCry1 in the presence of UV-p(dT)<sub>10</sub> with excitation at 532 nm (A) and 561 nm (B).

is not clear. It does not show any sensitivity to H/D-exchange,<sup>18,42</sup> which rules out that it involves a hydrogen bond donating group. Possibly, it is a marker for a hydrogen bond accepting group or a group that is sensitive to steric interactions in and/or polarity of the FADH• pocket.

Substrate binding causes a change in the weak band at 1351 cm<sup>-1</sup>, which shifts or completely disappears. Although this band is poorly resolved for FADH• in VcCry1, its behavior upon substrate binding is similar to that observed in PL upon substrate binding.<sup>18</sup> We interpret this shift as perturbation of the hydrogen-bonding interactions between the N<sub>3</sub>H and/or N<sub>5</sub>H of FADH• and the protein matrix upon substrate binding. The difference between the location of this band in substrate-free VcCry1 and PL and the change in its location upon substrate binding suggest that subtle differences in hydrogen bonding may contribute to the difference in the FADH<sup>-</sup>/FADH• reduction potential between VcCry1 and *E. coli* PL as well as to the change in this reduction potential upon substrate binding. This is similar to what we observed before in PL.<sup>18,20</sup>

**Thermodynamics of Substrate Binding.** Binding of damaged DNA to PL is relatively well understood with a number of studies published.<sup>23,28,43–50</sup> Sancar, Smith, and Sancar found that binding of PL to UV-damaged DNA was optimal at pH 7.4–7.6 with an ionic strength of 125 mM.<sup>28</sup> They also estimated that the binding of PL to undamaged DNA was at least 2 orders of magnitude less than for the damaged substrate. Using UV-irradiated pBr322 plasmid as substrate and the ionic strength described above, Sancar, Smith, Reid, et al. measured  $K_A = 5.7 (\pm 1.7) \times 10^7 \text{ M}^{-1}$  for PL in the FADH• state and  $4.8 \times 10^7 \text{ M}^{-1}$  for a sample described as 70% oxidized and 30% semiquinone PL.<sup>43</sup> We are unaware of any binding studies done with the CRY-DASH family.

Due to the large amount of substrate and the experimental conditions required for the ITC studies, we used UV-p(dT)<sub>10</sub> as our titrant. This substrate has nine unique ways of containing one CPD dimer in the molecule, assuming an equal probability of dimer formation between any two adjacent thymines. Using the algorithm described earlier<sup>23</sup> and assuming only one dimer per strand, we calculate a 22% chance that the dimer is located at the 3' or 5' end of the strand and a 78% chance that the dimer

is located internally. Based upon evidence in the literature with short oligonucleotides, we expect that substrate with damage on the end of the strand will bind less tightly than substrate with the CPD internal to the strand.

In addition, we were unable to obtain any ITC data using the buffer described as optimal for binding<sup>28</sup> since PL readily oxidizes and denatures in this buffer system. We used a 1240 mM ionic strength buffer (Buffer M) since both enzymes show exceptional resistance to denaturation and oxidation (PL specifically) in this buffer, but the high salt may impair binding.<sup>43</sup> The ITC method does allow us to assay the protein absorption spectra prior to and after our binding studies to quantify the oxidation and denaturation state of the enzyme after the experiment.

We find smaller association constants for the FADH• state of PL than previously reported, but since we use the same conditions for both enzymes we are able to compare PL and VcCry1 binding thermodynamics directly, Table 1. We found one major difference between VcCry1 and PL; our binding curve, Figure 6D, for the VcCry1 FADH• with double-stranded substrate appears to indicate that the VcCry1 is able to disrupt the double-stranded structure of a short strand of DNA. This result explains our activity assay result obtained with the dsDNA substrate where we did see apparent activity of VcCry1, in contrast to earlier reports.<sup>9,10</sup> The interaction between VcCry1 and UV-p(dT)<sub>10</sub> is more favorable than the interaction between the UV-p(dT)<sub>10</sub> and p(dA)<sub>10</sub>.

Some other trends are readily apparent with both enzymes. First, the association constant decreases by roughly 30% as the oxidation state of the protein is changed from FADH• to FAD<sub>ox</sub> for both systems, and the binding is less exothermic with oxidized protein. Both enzymes bind undamaged DNA at least two orders magnitude weaker than damaged substrate, in agreement with earlier observations.<sup>28</sup> PL binds ssDNA substrate significantly stronger and more exothermically than VcCry1, regardless of the oxidation state; PL can discriminate between damaged and undamaged DNA better.

A review by Jen-Jacobson contains a compilation of binding constants for protein binding to specific sites on DNA;<sup>51</sup> our binding constants of  $10^4 \text{ M}^{-1}$  and  $10^5 \text{ M}^{-1}$  are on the low end

of this range. The paper also reports the ratio of specific to nonspecific binding; there are a number of systems with reported ratios of  $10^2$ – $10^3$ , in the same range that we find for VcCry1 and PL. Therefore, although our binding constants are low, they are in line with other site-specific proteins based upon their ability to discriminate between specific and nonspecific binding.

The enthalpy of substrate binding is influenced by a number of factors: formation of specific contacts between the protein and DNA, desolvation of surfaces at the interface, and strain in the complex. Significant distortion of the DNA may lead to positive enthalpy of binding, while little or no distortion of the DNA may lead to negative enthalpy of binding.<sup>52</sup> The entropy of binding also may provide some insight since release of water and/or ions from the interface that forms between the molecules would be entropically favorable while loss of translational and rotational freedoms of the protein and DNA along with vibrational and conformational restrictions for all the species would be entropically unfavorable. In both PL and VcCry1, the enthalpy is favorable for all substrates and oxidation states, but PL has twice as much heat released as VcCry1. Regardless of substrate or oxidation state, the entropy of binding is favorable for both enzymes, but it is slightly higher for VcCry1.

Brudler, Hitomi, Daiyasu, Toh, et al. report that the cavity where the DNA binds is wider and shallower in CRY-DASH compared to PL.<sup>7</sup> Huang, Baxter, Smith, Partch, et al. report that the residues interacting with the CPD-containing DNA strand are strongly conserved in PL and CRY-DASH, but the residues that interact with the complementary strand of DNA are not conserved.<sup>11</sup> In addition, the cavity surface where CPD binds in AtCry3 is modified from what is seen with PL to more charge and less hydrophobic character, and they speculate that the alteration of the cavity polarity may significantly decrease the binding energy between the CPD and the CPD-binding cavity in AtCry3 relative to PL.<sup>11</sup> Pokorny, Klar, Hennecke, Carell, et al. published the only crystal structure of a CRY-DASH with synthetic CPD analogue bound, and they report that the binding mode of the thymine pair within the CPD binding cavity is very similar between CRY-DASH and PL, but the CRY-DASH cavity binds six structurally conserved water molecules along with being more polar.<sup>10</sup>

A wider DNA binding cavity in the CRY-DASH proteins would indicate that a greater surface area of protein may need to lose waters and ions upon binding the DNA molecule to the protein; this process would be enthalpically unfavorable and entropically favorable. The loss of hydrophobicity in the CPD-binding cavity could also lead to a weaker van der Waals interaction between the CPD and the protein, also less enthalpically favorable. Our ITC data is consistent with the structural information provided by the crystal structures.

One of more interesting outcomes of the ITC study was the large exothermic heat of dilution that we measured for oxidized VcCry1 protein. We followed up with an experiment to determine if this large enthalpy could be attributed to a dissociation of a VcCry1 dimer. We titrated concentrated oxidized VcCry1 into buffer and fit the resulting data to a dissociation model (data not shown). The exothermic dilution effect may be explained by dissociation of a dimer with a  $K_D$  of 0.8 ( $\pm 0.8$ ) mM and an enthalpy of dissociation of  $-2$  ( $\pm 1$ )  $\times 10^4$  cal/mol. A dissociation constant of this size means that approximately 20% of the oxidized VcCry1 protein would be in the dimer form at the concentrations used during the ITC experiments.

A recent paper by Sang, Li, Rubio, Zhang, et al. indicated that AtCry1, a plant cryptochrome, homodimerizes in a light-

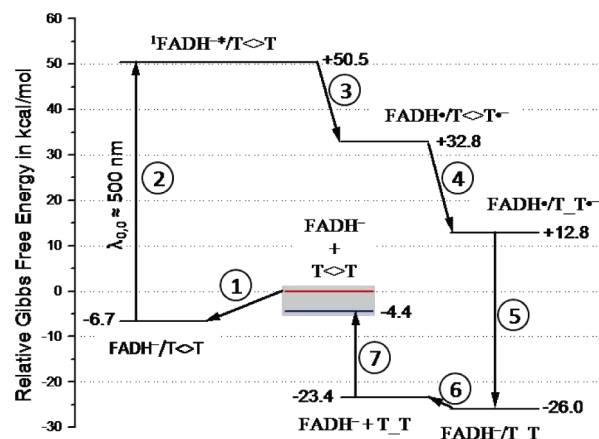


**Figure 8.** Proposed thermodynamic cycle of the photolyase and DNA system. The cycle takes into account the following steps: (1) substrate binding to PL, (2) excitation of FADH<sup>-</sup> to <sup>1</sup>FADH<sup>\*</sup>, (3) electron transfer from <sup>1</sup>FADH<sup>\*</sup> to T <> T, (4) reductive cleavage of T <> T<sup>•-</sup> to T<sup>•-</sup>T<sup>•-</sup>, (5) back electron transfer from T<sup>•-</sup>T<sup>•-</sup> to FADH<sup>•</sup>, (6) dissociation of the repaired DNA from PL, and (7) formation of the T <> T lesion. The red and blue lines indicate the start and end point of the cycle, respectively. All energies are in kcal/mol. The text provides more detail about the determination of the specific energies.

independent manner, the N-terminal domain is required for the dimerization, and the dimerization is required for activity.<sup>53</sup> They were able to detect the dimerization with *in vivo* chemical cross-linking but not with non-denaturing gels, implying that the association may be relatively weak. They found the dimerization was still present after illumination with blue light; blue light should cause the photoreduction of the oxidized flavin to FADH<sup>•</sup>.<sup>54</sup> This is inconsistent with our ITC result which was only observed with the fully oxidized form of VcCry1 and not the semiquinone form; the dimerization could simply be an artifact of the high concentrations used for the ITC studies and may lack physiological relevance.

**Thermodynamic Cycle of DNA Repair.** The reduction potentials and binding constants we obtained allow for a closer look at the thermodynamic cycle of DNA repair by PL, and our model is based upon earlier work by Heelis and co-workers.<sup>55</sup> The starting point of the cycle in Figure 8 is substrate-free enzyme and damaged DNA with a Gibbs free energy set to zero kcal/mol; all other energies will be given relative to this state. For the reduction potentials of the CPD and thymidine (dT), we will use the values that have been obtained in studies of model compounds dimethylthymine (DMT) and its dimer (DMTD) in polar and nonpolar solvents. The  $E^{\circ}(\text{DMT}^{\bullet-}/\text{DMT})$  is  $-2.14$  V (vs NHE) in acetonitrile, while the  $E^{\circ}$  for thymine and thymidine is  $-1.10$  V in aqueous solution.<sup>56,57</sup> The  $E^{\circ}(\text{DMTD}^{\bullet-}/\text{DMTD}) = -2.20$  V in acetonitrile,<sup>56</sup> and thymine dimers in aqueous solution may have  $E^{\circ} > -1.9$  V.<sup>58</sup> Studies by Falvey and co-workers on model compounds in acetonitrile and methanol found that hydrogen bonding can increase reduction potentials by 400 mV.<sup>58</sup> A value of  $E^{\circ}(\text{DMTD}^{\bullet-}/\text{DMTD}) = -2.62$  V has been reported in DMF but is based only on the  $E_p$  value of the cyclovoltammetric measurement.<sup>60</sup> X-ray crystallographic studies have indicated that the CPD binding pocket is part polar and part hydrophobic, and the CPD forms hydrogen bonds with the protein matrix and the FAD cofactor.<sup>40,61</sup> Therefore, we assume  $E^{\circ}(\text{DMTD}^{\bullet-}/\text{DMTD}) = -1.65$  V (the average of  $-2.20$  and  $-1.10$  V) is a reasonable approximation for that of the CPD in its binding pocket.

The binding of substrate to PL (step 1 in Figure 8) is accompanied by a  $\Delta G^{\circ} = -6.7$  kcal/mol as determined for UV-

p(dT)<sub>10</sub>. Electronic excitation of FADH<sup>-</sup> followed by relaxation to its lowest singlet excited state, <sup>1</sup>FADH<sup>-\*</sup>, raises the Gibbs free energy by +57.2 kcal/mol (step 2) as determined by the emission wavelength, λ<sub>0,0</sub>, of about 500 nm.<sup>62</sup> The change in Gibbs free energy for electron transfer from a photoexcited donor (D) to an acceptor (A) in kcal/mol is given by<sup>63</sup>

$$\Delta G_{\text{ET}} = 23.06[E^{\circ}(\text{D}^{\bullet+}/\text{D}) - E^{\circ}(\text{A}/\text{A}^{\bullet-}) - e^2/\epsilon a] - E_{0,0} \quad (1)$$

where  $E_{0,0}$  accounts for the energy gained from the photoexcitation process, and the term  $e^2/\epsilon a$  accounts for the free energy that is involved in bringing the two radical ions together to encounter distance  $a$  in a solvent of dielectric  $\epsilon$ . In the case of PL (and VcCry1), the FAD cofactor and the CPD never have a charge at the same time, and this Coulombic term is not taken into account. With  $E^{\circ}(\text{FADH}^-/\text{FADH}^{\bullet}) = 65$  mV in PL in the presence of substrate and  $E^{\circ}(\text{CPD}^{\bullet-}/\text{CPD}) = -1.65$  V, we find  $\Delta G_{\text{ET}} = -17.6$  kcal/mol for the forward electron transfer (step 3). Reductive cleavage of the CPD (step 4) has been estimated to have a  $\Delta G \approx \Delta H = -20$  kcal/mol.<sup>56</sup> For back electron transfer (BET) from dT<sup>•-</sup> to FADH<sup>•</sup> after repair (step 5), we make the same assumptions as for the forward electron transfer and use an average value of  $E^{\circ}(\text{dT}^{\bullet-}/\text{dT}) = -1.62$  V on the basis of the values determined for DMT.<sup>56,57,59</sup> In this case, the change in Gibbs free energy in kcal/mol is given by  $\Delta G_{\text{BET}} = 23.06[E^{\circ}(\text{dT}^{\bullet-}/\text{dT}) - E^{\circ}(\text{FADH}^-/\text{FADH}^{\bullet})] = -38.9$  kcal/mol. Dissociation of the repaired DNA from the enzyme (step 6) is accompanied by  $\Delta G^{\circ} = +2.6$  kcal/mol, as determined in this work. By taking into account all these processes, the state of PL plus repaired DNA is 23.4 kcal/mol lower in Gibbs free energy than the state of PL and damaged DNA. Part of the difference has to be accounted for by the energy change involved in damaging the DNA (step 7), which has been estimated to be  $\Delta G_{\text{damage}} \approx \Delta H_{\text{damage}} = +19$  kcal/mol.<sup>56</sup> Therefore, after completing the cycle, the system (PL and damaged DNA) ends up 4.4 kcal/mol below the starting point; this difference is not significant given the considerable uncertainty that yet exists for some of the steps involved in the process. Furthermore, it indicates that the assumptions that we have made about the reduction potentials of CPD and dT in the photolyase binding pocket were reasonable. Finally, the important contribution of our current and previous work on the determination of  $E^{\circ}(\text{FADH}^-/\text{FADH}^{\bullet})$  and the association and dissociation constants for p(dT)<sub>10</sub> and UV-p(dT)<sub>10</sub> has provided more realistic values for steps 1, 3, and 6 in the proposed thermodynamic cycle.

**Implications for DNA Repair.** One of the main concerns previously voiced was the similarity of the free energy changes for forward electron transfer from <sup>1</sup>FADH<sup>-\*</sup> to the CPD and charge recombination between CPD<sup>•-</sup> and FADH<sup>•</sup> without CPD repair.<sup>55</sup> This would indicate similar rates for these two processes, which suggests a competition between charge recombination and CPD repair and a relatively low quantum yield for DNA repair compared to experimentally established values. This inconsistency was mainly due to the estimated value of the FADH<sup>-</sup>/FADH<sup>•</sup> reduction potential (-330 to -500 mV).<sup>58</sup> Our previous and current work establishes a significantly higher (more positive) value for this reduction potential. Using the values for  $E^{\circ}(\text{FADH}^-/\text{FADH}^{\bullet})$  and  $E^{\circ}(\text{CPD}^{\bullet-}/\text{CPD})$  as discussed above, the free energy change for electron transfer from <sup>1</sup>FADH<sup>-\*</sup> to CPD could range from -4.95 kcal/mol (-0.21 eV) to -30.1 kcal/mol (-1.31 eV) in non-hydrogen-bonding and hydrogen-bonding environments of the CPD,

respectively. The free energy change for charge recombination between CPD<sup>•-</sup> to FADH<sup>•</sup> without CPD repair would range from -52.3 kcal/mol (-2.27 eV) to -26.8 kcal/mol (-1.17 eV) in non-hydrogen-bonding and hydrogen-bonding environments of the CPD, respectively. Using the average value of  $E^{\circ}(\text{DMTD}^{\bullet-}/\text{DMTD})$  for  $E^{\circ}(\text{CPD}^{\bullet-}/\text{CPD})$ , we find  $\Delta G = -17.6$  kcal/mol (-0.76 eV) and  $\Delta G = -39.4$  kcal/mol (-1.72 eV) for forward electron transfer and unproductive charge recombination, respectively. A reasonable value for the reorganization energy,  $\lambda$ , in biological electron transfer is 0.74 eV.<sup>64,65</sup> This implies that forward electron transfer is nearly activationless ( $-\Delta G = \lambda$ ) and occurs near the optimal rate, while unproductive charge recombination without repair takes place in the Marcus inverted region and will be significantly slower.<sup>66</sup> Experiments by the Stanley group have shown that forward electron transfer occurs with a rate of  $3.1 (\pm 1.9) \times 10^{10} \text{ s}^{-1}$  and that CPD repair starts within 60 ps ( $1.6 \times 10^{10} \text{ s}^{-1}$ ).<sup>67</sup> A similar fast rate of forward electron transfer was later confirmed by others.<sup>68</sup> Back electron transfer after CPD repair occurs with a time constant of 1.5–2 ns ( $6.7\text{--}5.0 \times 10^8 \text{ s}^{-1}$ ).<sup>67–69</sup> Since the reduction potential of DMT<sup>•-</sup>/DMT (a model for thymidine) is very similar to that of DMTD<sup>•-</sup>/DMTD,<sup>56,58</sup> the rate of unproductive charge recombination would be similar to that of back electron transfer after CPD repair. Our analysis is consistent with the evidence that unproductive charge recombination occurs at a much slower rate than forward electron transfer ( $(6.7\text{--}5.0) \times 10^8 \text{ s}^{-1}$  vs  $3.1 \times 10^{10} \text{ s}^{-1}$ ) and predicts a high quantum yield of DNA repair in agreement with the well-established experimental findings.<sup>4</sup>

## Conclusions

Our experiments mostly support the role of the CRY-DASH family as a single-strand DNA photolyase. The VcCry1 FADH<sup>-</sup>/FADH<sup>-</sup> reduction potential is 165 mV higher than that observed for PL but 300 mV higher than the value measured for the plant cryptochromes.<sup>14</sup> The enzyme repairs ssDNA with the same efficiency as PL, and the Raman spectrum of VcCry1 FADH<sup>•</sup> is very similar to that of PL, indicating similarities in the FAD binding pocket. We find that the VcCry1 enzyme is unable to directly bind dsDNA although it is able to displace the complementary strand and bind the ssDNA. There are some anomalies between the PL and VcCry1 enzymes: the enthalpy and entropy of ssDNA binding to VcCry1 is slightly modified from that of PL. In addition, oxidized VcCry1 has a large exothermic heat of dilution that may indicate the presence of a dimer, and the oxidation of the FADH<sup>•</sup> state occurs more readily in VcCry1 enzyme which may indicate a role for the FAD<sub>ox</sub> state. These new values for the reduction potential and for the binding constants also support a comprehensive thermodynamic cycle for CPD photolyase.

**Acknowledgment.** Y.M.G. is grateful for support from the National Science Foundation (CHE-0922712) and the Department of Chemistry at Lafayette College. K.S., M.N., J.F., and J.C. acknowledge support from the Lafayette ARC for the EXCEL scholars and travel funding. J.P.M.S. acknowledges support from the National Science Foundation (MCB-0920013). We gratefully acknowledge Dr. Aziz Sancar for the cell lines used in this work. We also acknowledge Dr. Chip Nataro for technical assistance in viewing crystal structures.

## References and Notes

- (1) Sancar, A. *J. Biol. Chem.* **2004**, *279*, 34079.
- (2) Cashmore, A. R. *Cell* **2003**, *114*, 537.

- (3) Partch, C. L.; Sancar, A. *Photochem. Photobiol.* **2005**, *81*, 1291.
- (4) Sancar, A. *Chem. Rev.* **2003**, *103*, 2203.
- (5) Losi, A. *Photochem. Photobiol.* **2007**, *83*, 1283.
- (6) Kay, C. W. M.; Bacher, A.; Fischer, M.; Richter, G.; Schleicher, E.; Weber, S. *Photochem. Photobiol. Sci.* **2006**, *6*, 151.
- (7) Brudler, R.; Hitomi, K.; Daiyasu, H.; Toh, H.; Kucho, K.; Ishiura, M.; Kanehisa, M.; Roberts, V. A.; Todo, T.; Tainer, J. A.; Getzoff, E. D. *Mol. Cell* **2003**, *11*, 59.
- (8) Daiyasu, H.; Ishikawa, T.; Kuma, K.; Iwai, S.; Todo, T.; Toh, H. *Genes Cells* **2004**, *9*, 479.
- (9) Selby, C. P.; Sancar, A. *Proc. Natl. Acad. Sci. U.S.A.* **2006**, *103*, 17696.
- (10) Pokorny, R.; Klar, T.; Hennecke, U.; Carell, T.; Batschauer, A.; Essen, L.-O. *Proc. Natl. Acad. Sci.* **2008**, *105*, 21023.
- (11) Huang, Y.; Baxter, R.; Smith, B. S.; Partch, C. L.; Cobert, C. L.; Deisenhofer, J. *Proc. Natl. Acad. Sci. U.S.A.* **2006**, *103*, 17701.
- (12) Klar, T.; Pokorny, R.; Moldt, J.; Batschauer, A.; Essen, L. O. *J. Mol. Biol.* **2007**, *366*, 954.
- (13) Worthington, E. N.; Kavakli, I., H.; Berrocal-Tito, G.; Bondo, B.; Sancar, A. *J. Biol. Chem.* **2003**, *278*, 39143.
- (14) Balland, V.; Byrdin, M.; Eker, A. P. M.; Ahmad, M.; Brettel, K. *J. Am. Chem. Soc.* **2009**, *131*, 426.
- (15) Song, S.-H.; Dick, B.; Penzkofer, A.; Pokorny, R.; Batschauer, A.; Essen, L.-O. *J. Photochem. Photobiol.* **2006**, *85*, 1.
- (16) Zikihara, K.; Ishikawa, T.; Todo, T.; Tokutomi, S. *Photochem. Photobiol.* **2008**, *84*, 1016.
- (17) Damiani, M. J.; Yalloway, G. N.; Lu, J.; McLeod, N. R.; O'Neill, M. A. *Biochemistry* **2009**, *48*, 11399–11411.
- (18) Schelvis, J. P. M.; Ramsey, M.; Sokolova, O.; Tavares, C.; Cecala, C.; Connell, K.; Wagner, S.; Gindt, Y. M. *J. Phys. Chem. B* **2003**, *107*, 12352.
- (19) Gindt, Y. M.; Schelvis, J. P. M.; Thoren, K. L.; Huang, T. H. *J. Am. Chem. Soc.* **2005**, *127*, 10472.
- (20) Murphy, A. K.; Tamaro, M.; Cortazar, F.; Gindt, Y. M.; Schelvis, J. P. M. *J. Phys. Chem. B* **2008**, *112*, 15217.
- (21) Sokolova, O.; Cecala, C.; Gopal, A.; Cortazar, F.; McDowell-Buchanan, C.; Sancar, A.; Gindt, Y. M.; Schelvis, J. P. M. *Biochemistry* **2007**, *46*, 3673.
- (22) Gindt, Y. M.; Vollenbroek, E.; Westphal, K.; Sackett, H.; Sancar, A.; Babcock, G. T. *Biochemistry* **1999**, *38*, 3857.
- (23) Jorns, M. S.; Sancar, G. B.; Sancar, A. *Biochemistry* **1985**, *24*, 1856.
- (24) Eisenberg, A. S.; Schelvis, J. P. M. *J. Phys. Chem. A* **2008**, *112*, 6179.
- (25) Jorns, M. S.; Sancar, G. B.; Sancar, A. *Biochemistry* **1984**, *23*, 2673.
- (26) Wang, B.; Jorns, M. S. *Biochemistry* **1989**, *28*, 1148.
- (27) Dutton, P. L. *Methods Enzymol.* **1978**, *54*, 411.
- (28) Sancar, G. B.; Smith, F. W.; Sancar, A. *Biochemistry* **1985**, *24*, 1849.
- (29) Murgida, D. H.; Schleicher, E.; Bacher, A.; Richter, G.; Hildebrandt, P. *J. Raman Spectrosc.* **2001**, *32*, 551.
- (30) Li, J.; Uchida, T.; Todo, Y. M.; Kitagawa, T. *J. Biol. Chem.* **2006**, *281*, 25551.
- (31) Sawyer, D. T.; Sobkowiak, A.; Roberts, J. L. *Electrochemistry for Chemists*; John Wiley & Sons: New York, 1995; p 192.
- (32) DeRosa, M. C.; Sancar, A.; Barton, J. K. *Proc. Natl. Acad. Sci. U.S.A.* **2005**, *102*, 10788.
- (33) Lin, C.; Robertson, D. E.; Ahmad, M.; Raibekas, A. A.; Jorns, M. S.; Dutton, P. L.; Cashmore, A. R. *Science* **1995**, *269*, 968.
- (34) Swenson, R. P.; Krey, G. D. *Biochemistry* **1994**, *33*, 8505.
- (35) Pellet, J. D.; Sabaj, K. M.; Stephens, A. W.; Bell, A. F.; Wu, J.; Tonge, P. J.; Stankovich, M. T. *Biochemistry* **2000**, *29*, 13982.
- (36) Breinlinger, E.; Niemz, A.; Rotello, V. M. *J. Am. Chem. Soc.* **1995**, *117*, 5379.
- (37) Cuello, A. O.; McIntosh, C. M.; Rotello, V. M. *J. Am. Chem. Soc.* **2000**, *122*, 3517.
- (38) Breinlinger, E. C.; Rotello, V. M. *J. Am. Chem. Soc.* **1997**, *119*, 1165.
- (39) Walsh, J. D.; Miller, A.-F. *J. Mol. Struct.: THEOCHEM* **2003**, *623*, 185.
- (40) Mees, A.; Klar, T.; Gnau, P.; Hennecke, U.; Eker, A. P. M.; Carrell, T.; Essen, L.-O. *Science* **2004**, *306*, 1789.
- (41) Immeln, D.; Schlesinger, R.; Heberle, J.; Kottke, T. *J. Biol. Chem.* **2007**, *282*, 21720.
- (42) Li, J.; Uchida, T.; Ohta, T.; Todo, T.; Kitagawa, T. *J. Phys. Chem. B* **2006**, *110*, 16724.
- (43) Sancar, G. B.; Smith, F. W.; Reid, R.; Payne, G.; Levy, M.; Sancar, A. *J. Biol. Chem.* **1987**, *262*, 478.
- (44) Husain, I.; Sancar, A. *Nucleic Acids Res.* **1987**, *15*, 1109.
- (45) Husain, I.; Sancar, G. B.; Holbrook, S. R.; Sancar, A. *J. Biol. Chem.* **1987**, *262*, 13188.
- (46) Jordan, S. P.; Jorns, M. S. *Biochemistry* **1988**, *27*, 8915.
- (47) Jordan, S. P.; Alderfer, J. L.; Chanderkar, L. P.; Jorns, M. S. *Biochemistry* **1989**, *28*, 8149.
- (48) Baer, M.; Sancar, G. B. *Mol. Cell. Biol.* **1989**, *9*, 4777.
- (49) Kim, S.; Sancar, A. *Biochemistry* **1991**, *30*, 8623.
- (50) Baer, M. E.; Sancar, G. B. *J. Biol. Chem.* **1993**, *268*, 16717.
- (51) Jen-Jacobson, L. *Biopolymers* **1997**, *44*, 153.
- (52) Jen-Jacobson, L.; Engler, L. E.; Jacobson, L. A. *Structure* **2000**, *8*, 1015.
- (53) Sang, Y.; Li, Q.-H.; Rubio, V.; Zhang, Y.-C.; Mao, J.; Deng, X.-W. *Plant Cell* **2005**, *17*, 1569.
- (54) Bouly, J. P.; Schleicher, E.; Dionisio-Sese, M.; Vandebussche, F.; Van Der Staeten, D.; Bakrim, N.; Meier, S.; Batschauer, A.; Galland, P.; Bittl, R.; Ahmad, M. *J. Biol. Chem.* **2007**, *282*, 9383.
- (55) Heelis, P. F.; Hartman, R. F.; Rose, S. D. *Chem. Soc. Rev.* **1995**, *24*, 289.
- (56) Scannell, M. P.; Fenick, D. J.; Yeh, S.-R.; Falvey, D. E. *J. Am. Chem. Soc.* **1997**, *119*, 1971.
- (57) Steenken, S.; Telo, J. P.; Novais, H. M.; Candeias, L. P. *J. Am. Chem. Soc.* **1992**, *114*, 4701.
- (58) Heelis, P. F.; Deeble, D. J.; Kim, S.-T.; Sancar, A. *Int. J. Radiat. Biol.* **1992**, *62*, 137.
- (59) Scannell, M. P.; Prakash, G.; Falvey, D. E. *J. Phys. Chem. A* **1997**, *101*, 4332.
- (60) Boussicault, F.; Krüger, O.; Robert, M.; Wille, U. *Org. Biomol. Chem.* **2004**, *2*, 2742.
- (61) Park, H.-W.; Kim, S.-T.; Sancar, A.; Deisenhofer, J. *Science* **1995**, *268*, 1866.
- (62) Jorns, M. S.; Wang, B.; Jordan, S. P. *Biochemistry* **1987**, *26*, 6810.
- (63) Rehm, D.; Weller, A. *Isr. J. Chem.* **1970**, *8*, 259.
- (64) Gray, H. B.; Winkler, J. R. *Q. Rev. Biophys.* **2003**, *36*, 341.
- (65) Page, C. C.; Moser, C. C.; Chen, X.; Dutton, P. L. *Nature* **1999**, *402*, 47.
- (66) Marcus, R. A.; Sutin, N. *Biochim. Biophys. Acta* **1985**, *811*, 265.
- (67) MacFarlane, A. W., IV; Stanley, R. J. *Biochemistry* **2003**, *42*, 8558.
- (68) Kao, Y.-T.; Saxena, C.; Wang, L.; Sancar, A.; Zhong, D. *Proc. Natl. Acad. Sci. U.S.A.* **2005**, *102*, 116128.
- (69) Okamura, T.; Sancar, A.; Heelis, P. F.; Begley, T. P.; Hirata, Y.; Mataga, N. *J. Am. Chem. Soc.* **1991**, *113*, 3143.